Available online at www.sciencedirect.com

ScienceDirect

Energy Procedia 49 (2014) 1439 – 1449

Energy Procedia

SolarPACES 2013

Design and testing of a novel air-cooled condenser for concentrated solar power plants

J. Moore[1], R.Grimes[1], A. O'Donovan[1], E. Walsh[2]

[1] *Stokes Research Institute, University of Limerick, Castletroy, Limerick, Ireland*

[2] *Osney Thermo-Fluids Laboratory, University of Oxford, Oxford,UK*

Abstract

This paper aims at developing a novel air-cooled condenser for concentrated solar power plants. The condenser offers two significant advantages over the existing state of the art. Firstly, it can be installed in a modular format where pre-assembled condenser modules reduce installation costs. Secondly, instead of using large, fixed speed fans, smaller speed controlled fans are incorporated into the individual modules. This facility allows the operating point of the condenser to change in order to maximise plant efficiency at all times. Two condenser designs were proposed and full-scale prototype modules were manufactured for experimental testing. Both designs comprise a bank of circular finned tubes, coupled to an array of axial fans. The air-side thermal and aerodynamic characteristics were measured using a purpose built steady-state test facility. The measurements were correlated and compared well with existing correlations in the relevant literature, thus validating their use in thermodynamic models to predict power plant performance. A plant performance analysis was conducted combing the experimental measurements with output data from a 50MW concentrated solar power plant. This analysis firstly verified that the plant efficiency can be continually maximised by altering the condenser fan speed. Furthermore, under certain conditions plant output can be increased by over 10% by varying fan speed by 10% of the full speed. The study also provides a comparison of the two designs in terms of their effect on the plant output power. With respect to the thermodynamic efficiency and cost-efficiency, the four row condenser substantially outperforms the initial six row design.

Selection and peer review by the scientific conference committee of SolarPACES 2013 under responsibility of PSE AG.

Final manuscript published as received without editorial corrections.

Keywords: Air cooled condenser; Air cooled heat exchanger; CSP plant performance analysis

1. Introduction

Air-Cooled condensers can potentially reduce the water consumption of a power plant by up to 90%. This is particularly significant for Concentrated Solar Power (CSP) plants which are typically located in extremely dry

Selection and peer review by the scientific conference committee of SolarPACES 2013 under responsibility of PSE AG.

Final manuscript published as received without editorial corrections.

doi:10.1016/j.egypro.2014.03.153

regions, where water for wet cooling systems is limited. In many cases an air-cooled condenser may be the only feasible option for a CSP plant. However, the high operating costs and corresponding hit on plant efficiency associated with an air-cooled condenser makes it an unpopular option, and there is a clear requirement for more efficient dry cooling systems for CSP plants. This is seen as a significant barrier to the development of CSP plants in many regions around the world. This paper is aimed towards the development of a novel air-cooled condenser which can be erected in a modular format and thus sized for any CSP plant.

Nomenclature

A	heat transfer area (m^2)	h	heat transfer coefficient (W/m^2K)
A_o	free flow area (m^2)	h_{fg}	enthalpy of vaporisation (kJ/Kg)
C_{alum}	cost per unit mass of aluminium ($)	$\dot{m}$	mass flow rate (Kg/s)
Cc	cost ($)	p	pressure (Pa)
C_{steel}	cost per unit mass of steel ($)	r_h	hydraulic radius, A_oL/A (m)
D	fan diameter (m)	u	velocity (m/s)
G	mass velocity (Kg/m^2)		
L	condenser depth (in direction of the flow) (m)	*Dimensionless numbers*	
M	mass (Kg)	f	friction factor
N	fan speed (rpm)	Re	Reynolds number
N_f	number of fins per meter	Pr	Prandtl number
P_{fan}	power (W)	St	Stanton number $h/c_p\rho u$
Q	heat power (W)		
S_d	diagonal tube pitch (m)	*Greek letters*	
S_f	$1/N_f$	δ	fin thickness
St	transverse tube pitch (m)	ε	effectiveness
T	temperature (K)	η_{loss}	efficiency loss
		μ	dynamic viscosity (Kg/m s)
c_{min}	minimum capacity rate (W/K)	ρ	density (Kg/m^3)
c_p	specific heat capacity (kJ/KgK)		
d_e	fin diameter (m)		
d_h	hydraulic diameter, $4r_h$ (m)		
d_o	tube exterior diameter (m)		

The current state of the art in ACCs consists of a series of plate finned, rectangular tubes coupled with very large axial fans usually operated at a constant speed. These condensers have a number of inherent design issues and the fact that the fans, usually operate at a constant speed means that the condenser usually operates at one point only and cannot adapt to an optimum operating point given the changing ambient conditions. Walsh et al. [1] reported a number of these issues. The proposed Modular Air-Cooled Condenser (MACC) design considers the heat sink and fan array as a composite solution and employs much smaller speed controlled fans. Additionally, it is envisioned that the condenser and fan array be incorporated into a pre-assembled module and instead of erecting the very large existing ACC structures, that an array of smaller modules be installed. It is expected that this concept will offer significant installation cost savings. This paper focuses on the air-side performance of the condenser as this is the dominant thermal resistance, particularly determining the appropriate balance between heat transfer and pressure drop and the effect of various design parameters on the performance of a CSP plant.

Two full-scale prototype MACCs were manufactured and experimentally tested to characterise the air-side thermal and aerodynamic performance. Both prototype designs comprise a circular finned tube bank coupled with an array of axial fans. The modules were both square in shape with a face area of four meters squared. The initial design contained six rows of equilaterally staggered steel tubes which had thin exterior aluminium fins attached in a helical pattern. The second design contained four rows of the same tubes arranged in the same manner. Zukauskas

[2], Nir [3] and Gianolio and Cuti [4] have all reported that reducing the number of tube rows has a diminishing effect on heat transfer, due to a reduction in turbulence levels throughout the core flow. In a similar investigation the authors [5] also reported on this topic. While heat transfer may deteriorate, the flow resistance is significantly reduced by reducing the condenser tube rows from six to four. This leaves potential for the four row design to have a higher heat to power ratio. Another reason to reduce the number of tube rows is due to the phenomenon of backflow, an inherent issue with a multi-row condenser design which is explained in further detail in [5] and [6]. Both condenser designs were characterised for two fan scenarios, the fans forcing the air through the condenser (forced draft, FD) and the fans inducing the flow through the condenser (induced draft, ID). Both scenarios have very different flow field attributes which can have an effect on both heat transfer and pressure drop. To the best knowledge of the authors, other than the measurements of [4], no other measurements of heat exchanger performance in realistic fan flows have been published, and the measurements of [9] were for a limited range of geometric parameters.

In order to compare the condenser designs, the experimental measurements were combined with plant output data from a 50MW concentrated solar power plant. A thermodynamic model was developed to calculate the thermodynamic performance of the plant with various condenser sizes, designs and also different ambient conditions. The results of this analysis show a primary advantage of the technology; irrespective of the condenser design, size or ambient conditions, there is an optimum fan speed which yields the maximum net output power. The variable speed fans can continuously adapt to maintain this speed, and hence achieve maximum possible plant efficiency at all times. While this will require tight fan speed control, it offers a significant advantage over the current state of the art.

The thermodynamic analysis highlights the trade-off between efficiency and the size of the condenser, i.e. the number of modules to be installed. Increasing the number of modules increases efficiency but also increases capital cost. An effort has therefore been made to conduct a cost-efficiency analysis. In order to estimate the capital cost of the condenser a number of manufacturers and industrial partners were consulted. A relationship to estimate the cost was developed and is presented in the paper. The relationship is based on a number of assumptions but for the purpose of a comparative analysis the authors deem it a reasonable means of cost estimation. The study shows that a condenser with fewer tube rows is an attractive option as it leads to a higher plant efficiency and also has less material, significantly reducing the capital costs. These thermodynamic and cost analyses provide a novel means of evaluating heat exchanger performance on the basis of effects on CSP plant performance.

2. Theory

In this section correlations from literature, which predict the air-side pressure drop and heat transfer in the various condenser designs are presented. Due to the chaotic nature of the flow field over the circular finned tube bank only experimental correlations exist to predict the pressure drop and heat transfer. Equation (1) is the correlation of Robinson and Briggs [7] which was used to predict the dimensionless friction factor across a circular finned tube heat exchanger. The correlation is valid in the flow range of $2000 < Re < 50000$. Gianolio and Cuti [4], report that the number of rows has an insignificant effect on the accuracy of the pressure drop prediction of [7].

$$f = 9.465 Re^{-0.316} \left(\frac{S_t}{d_o}\right)^{-0.927} \left(\frac{S_t}{S_d}\right)^{0.515} \frac{n_r d_h}{L} \quad (1)$$

Where,

$$Re = \frac{d_o \dot{m}_a}{\mu A_o} \quad (2)$$

The relationship between the dimensionless friction factor and the pressure drop over a finned tube bank is presented in Equation (3) [8 9]. The equation accounts for the different phenomena which contribute to the overall pressure drop. In the case of the circular finned tube designs the inlet and exit losses due to sudden contraction and

expansion of the flow are combined in the correlated friction factor and so additional terms to account for these are not required.

$$\frac{\Delta p}{p_i} = \frac{G^2}{2g_c\rho_i p_i}\left[\underbrace{f\frac{L}{r_h}\rho_i\left(\frac{1}{\rho}\right)_m}_{core\ friction} + \underbrace{2\left(\frac{\rho_i}{\rho_o}-1\right)}_{momentum\ effect} \right] \tag{3}$$

The correlation of Briggs and Young [10] relates the Reynolds number of the flow with the Colburn factor, a non-dimensional heat transfer characteristic. The Colburn factor is the product of the Stanton number and Prandtl number to the power of two thirds. This correlation was used to predict the thermal performance of the circular finned tube condenser designs and is listed below in Equation (4). This correlation is valid within the flow range of $1100<Re<18000$.

$$StPr^{2/3} = 0.134Re^{0.319}\left[\frac{2(S_f-\delta_f)}{d_e-d_o}\right]^{0.2}\left(\frac{S_f-\delta_f}{\delta_f}\right)^{0.1134} \tag{4}$$

Equation (5) presents an additional correlation factor presented by Gianolio and Cuti [4], to be used with Equation (4) to compensate the reduction in heat transfer for reduced tube rows.

$$\frac{h_{n_r}}{h_6} = \left(1+\frac{u_o}{n_r^2}\right)^{-0.14} \tag{5}$$

Equations (6), (7) and (8) represent the three fan scaling laws [11 12] which can be used, together with pressure drop calculations from Equation (3), and fan manufacturer performance characteristics to determine the flow rate through a fan cooled heat exchanger and fan power consumption at a given fan speed.

$$\dot{V} \propto ND^3 \tag{6}$$

$$\Delta p \propto \rho N^2 D^2 \tag{7}$$

$$P_f \propto \rho N^3 D^5 \tag{8}$$

3. Experimental details

To characterize the air-side thermal and aerodynamic performance of the condenser designs, a steady state test facility which uses condensing steam inside the tubes of the test core was designed. The test methodology was similar to that employed by Kays and London [8, 13]. Using steam ensures the temperature to be uniform across the entire core. Furthermore by passing significantly more steam through the tube than can be condensed, the thermal resistance from the steam to the tube inner surface is minimized.

Figure 1 is a pictorial view of the prototype test facility. Suspended in the frame structure (5) is the prototype condenser (3) and each prototype can be coupled with the fan array (6). The fan array consists of four axial fans of 0.91m diameter. The test facility also allows the inclination and the fan to heat exchanger spacing to be varied. Steam is supplied to the inlet header (1) from an industrial steam boiler and passed through a series of valves to ensure it was in a superheated condition and slightly elevated above atmospheric pressure entering the condenser at (2). A positive pressure is essential to ensure air and other non-condensables do not enter the condenser which would create temperature non-uniformities. Providing steam in a superheated condition enables an accurate calculation of the enthalpy at inlet of the condenser. A maximum of five degrees superheat was tolerated as the corresponding change in enthalpy due to the sensible cooling is negligible compared to the enthalpy of vaporisation. Upon exit from the condenser at (7) the excess steam was separated from the condensate and vented away. The condensate was gathered, weighed and the time taken was recorded.

Pressure tappings (8) were fitted to the walls of the fan enclosure (4) to measure the air-side pressure drop across the condenser. Steam pressure was measured at the inlet and outlet header using absolute pressure transducers. Air temperatures were measured at the test core inlet and outlet to calculate necessary properties. The air temperature was measured with thermistors which were integrated into one arm of a Wheatstone bridge for higher sensitivity and noise rejection. Steam temperatures were measured using K-type thermocouples at certain points in the steam supply line as well as at the inlet and outlet headers. All instrumentation was synchronized with a LabView 2011 data acquisition VI.

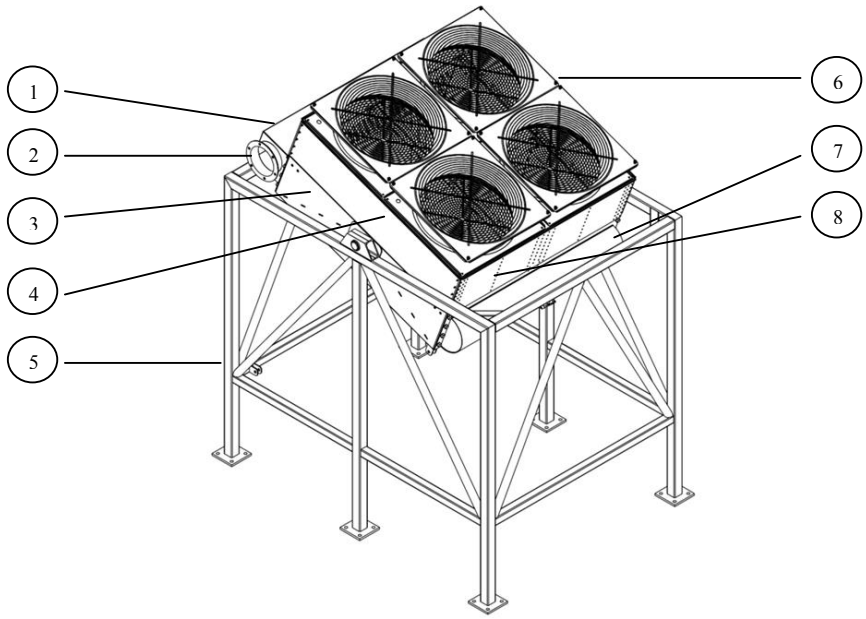

Figure 1. Pictorial view of the prototype test facility

4. Data reduction

4.1. Experimental data reduction

By applying an energy balance to the test system and ensuring that there was negligible sensible cooling of the steam or the condensate, the heat rejected by the condenser was equivalent to the product of the mass flow of condensate times the enthalpy of vaporization as indicated in Equation (9). The overall thermal conductance, U, was calculated from the measured heat rejection using Equation (10). The air-side heat transfer coefficient, h, can be extracted from U, using the thermal resistance method [2, 3, 14]. To extract h, the steam-side conductance is required but as the steam-side resistance is generally 5-10% of the total resistance in such a test scenario, an estimate of h_c will suffice [13]. The remaining terms in Equation (11) are constants apart from η_o, the air-side surface effectiveness. This is dominated by the fin effectiveness, which from the work of Gardner [15], can be calculated using Equation (12). The overall surface effectiveness, η_o, is a weighted average of the effectiveness of the prime surface and less than 100% of the fin surface as described in Equation (13) [8]. The experimental heat transfer coefficient was expressed in non-dimensional form for comparison with literature. The pressure drop was directly measured using a digital monometer. The measured pressure drop was then expressed non-dimensionally using Equation (3).

$$Q_{rej} = \dot{m}_c h_{fg} \tag{9}$$

$$\epsilon = 1 - e^{-\frac{UA}{C_{min}}} = \frac{\dot{m}_a c_p (T_{air\,out} - T_\infty)}{\dot{m}_a c_p (T_s - T_\infty)} = \frac{Q_{rej}}{\dot{m}_a c_p (T_s - T_\infty)} \tag{10}$$

Where,

$$\frac{1}{UA} = \frac{1}{\eta_o h A} + \frac{1}{h_c A_c} + \frac{\delta_w}{k_w A_w} \tag{11}$$

$$\eta_f = \frac{\tanh ml}{ml}; \quad m = \sqrt{\frac{2h}{k\delta}} \tag{12}$$

$$\eta_o = 1 - \frac{A_f}{A}\left(1 - \eta_f\right) \tag{13}$$

4.2. CSP plant analysis

The experimental measurements were used to conduct a performance analysis on a CSP plant. The aim of this analysis was to develop a thermodynamic model to calculate the effect of various condenser parameters on power plant output. Therefore, during the analysis, the only parameters which were varied were those relating to the condenser. All others, such as turbine inlet steam temperature and flow rate were kept at constant values, representative of those in a CSP plant steam turbine under typical conditions of solar radiation. Figure 2 presents performance characteristics from such a steam turbine operating in a CSP plant [16]. The plot relates the steam turbine gross output power and condenser heat rejection, to the turbine outlet steam temperature. As the condenser temperature increases, the condenser heat rejection also increases, causing a reduction in the steam turbine gross power output.

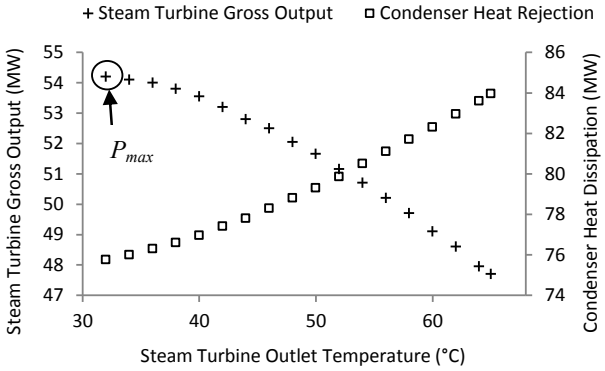

Figure 2. Steam turbine outlet temperature versus the steam turbine gross output power and condenser heat rejection of a CSP plant operating under typical conditions

Equation (14) governs the relationship between the condenser temperature, T_s, the condenser heat rejection, Q, and the heat transfer coefficient, h. Using the data in Figure 2 it was possible to express the condenser heat rejection as a function of the outlet steam temperature and use this relationship as an input to Equation (14). For a given fan speed, the flow rate and fan power consumption were calculated based on the fan performance curves using the fan laws, Equations (6), (7) and (8), and the system pressure drop curve determined using Equation (3). For a given flow rate the heat transfer coefficient was calculated using measurements and correlations presented in the following section. For any given condenser design, (i.e. the size and tube bank design) and ambient temperature, Equation (14) was solved for steam turbine outlet temperature and corresponding gross output power. The net power output was calculated by subtracting the total fan power consumption from the gross power output. This calculation procedure was repeated for various fan speeds, (which in turn varies heat transfer coefficient and fan power) various

condenser designs, (number of modules and tube bank design) and different ambient temperatures. The plant performance over a range of operational points was plotted for comparison of the various condenser designs.

$$\frac{Q}{\dot{m}c_p(T_s - T_\infty)} = 1 - e^{-\frac{hA}{C_{min}}} \tag{14}$$

Instead of expressing plant performance in terms of the net plant output, it may be more telling to express it in terms of efficiency loss due condenser performance as defined in Equation (15).

$$\eta_{loss} = \left(1 - \frac{P_{net}}{P_{max}}\right) \times 100\% \tag{15}$$

To complete a comparison of the prototype designs, a cost analysis was also required. In order to achieve this some assumptions were necessary. To predict the installation cost, a number of manufacturers and industrial partners were consulted and the following relationship, Equation (16), was determined to estimate the capital cost. The relationship is based on the cost per unit mass of the metals used in the respective design i.e. steel tubes and aluminium fins, the cost of the axial fans which is known and a conservative scaling factor of 5 which accounts for manufacture and installation.

$$Cc = \{[(M_{alum} \times C_{alum}) + (M_{steel} \times C_{steel})] \times 5\} + C_{fans} \tag{16}$$

5. Results and discussion

This section firstly presents the non dimensional pressure drop and heat transfer measurements as described in the preceding sections. These results were compared with the relevant theory and correlations which were presented in section 2. The two designs were then compared in terms of the effect on thermodynamic plant performance and also on a cost-efficiency basis.

5.1. Experimental results

Figure 3(a) presents the pressure drop results for the two condenser designs for both forced and induced draft air flows. The induced draft results show good agreement with the Robinson and Briggs [7] correlation with a 4.5% mean deviation for the four row design and 6.5% for the six row design. This is not surprising given that their data was measured in a uniform wind tunnel flow which is comparable to that produced in an induced draft scenario. The forced draft results do not match the correlated data as well and there are many possible factors which contribute to this. Certainly there is a higher pressure drop associated with the forced draft scenario due to flow separation from the fins as the swirling flow enters the core. However, pressure recovery also occurs as the radial component is removed from the flow as it straightens through the core. Some authors have reported on this phenomenon but few go into technical detail. Gianolio and Cuti [4] state that the conflicting phenomena cancel each other out and there is no significant difference between forced and induced draft scenarios. Meyer and Kroger [17] claim that in certain scenarios, pressure recovery is in fact greater than the additional pressure drop resulting in less fan power consumption. A greater issue in this case is accurately measuring the forced draft pressure drop. Due to the size of the test facility the only feasible means of measuring the pressure drop was using wall pressure tappings and this requires parallel streamlines of flow over the walls. While an induced draft flow will reasonably satisfy this condition it is certainly not the case for a forced draft flow where the flow has a high degree of swirl and is generally chaotic in both the radial and axial directions. However, the fan power consumption in both cases agreed well suggesting that the pressure recovery which occurred balances out with the increased pressure drop. This suggests good agreement with Gianolio and Cuti [4]. Further investigation is required to clarify this issue. For the forced draft measurements, the mean deviations from the correlation of [7] for the four row and six row designs were 18% and 25% respectively.

Figure 3(b) presents the experimental heat transfer results. The first point to note is that for both condenser designs the forced draft and induced draft results are in good agreement with each other. Due to the very different flow fields generated in each case this might be somewhat surprising. Gianolio & Cuti [4] report that this is due to similar turbulence levels generated in a six row and four row heat exchanger core regardless of the inlet flow field. In the induced draft scenario, turbulence is created as vortices shed from the tube and fin surfaces downstream of the first tube row. In the forced draft scenario, the first tube row may be subjected to higher turbulence than the induced draft case, but in a four or six row heat exchanger this does not result in a substantial overall heat transfer enhancement. The results confirm this and also show good agreement, approximately 5.9% mean deviation, with the correlations of Briggs and Young [10] and Gianolio and Cuti [4] verifying the use of both correlations for further analysis.

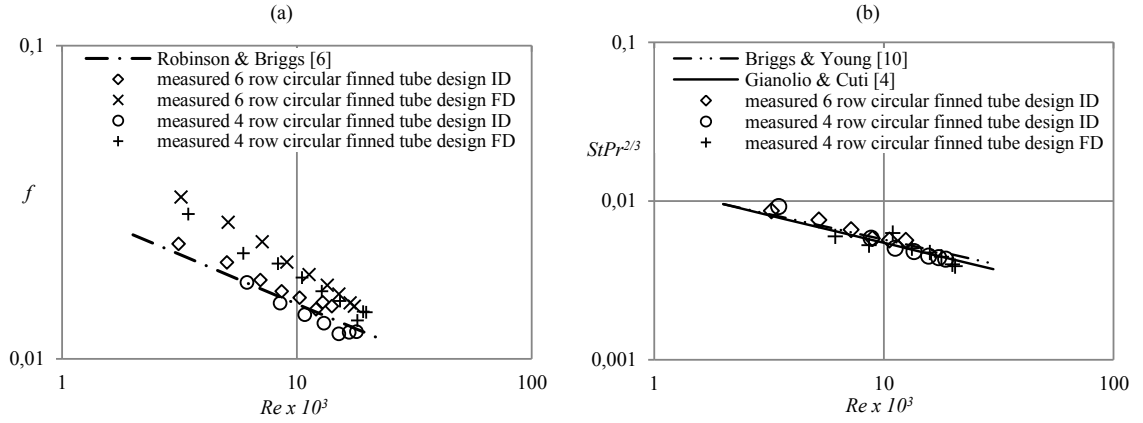

Figure 3. (a) A plot of friction factor against Reynolds number (b) A plot of the non-dimensional heat transfer against Reynolds number

5.2. CSP plant analysis results

Initially two condenser sizes were considered for the power plant analysis, 260 2m x 2m modules and 650 2m x 2m modules. These condenser sizes were selected somewhat arbitrarily, but nevertheless demonstrate the effect on plant output of increasing the number of modules. The number of modules may appear high but it is envisioned that the final design would be 2m x 8m modules and therefore reduce the amount by four. Figure 4 shows the performance of the plant in terms of net power output (P_{gross}-P_{fans}) for the two condenser sizes at a range of ambient temperatures. For each condenser the performance is plotted against fan speed for 10°C, 20°C and 30°C. It should be noted that Figure 4 is for the four row condenser and the results for the six row condenser have been omitted for clarity but follow a similar trend. This plot shows the primary advantage of the technology, by varying fan speed by just 100 rpm in some cases, an increase in plant performance of over 10% can be achieved. Despite the condenser size or the ambient temperature there exists an optimum fan speed which yields the maximum net output power. Below this optimum, increasing the fan speed has the effect of reducing the turbine back pressure and hence increasing the gross turbine power by a greater magnitude than the increase in fan power. Above the optimum, further fan speed increases will continue to reduce the turbine back pressure but the increase in fan power is greater than the corresponding increase in gross turbine power. Increasing ambient temperature results in an increase in the optimum fan speed, and fan speed should always be adjusted to this optimum. Increasing the size of the condenser causes a reduction of the optimum fan speed at any given ambient temperature.

The plot in Figure 5 is an expansion of the thermodynamic analysis presented in Figure 4 and compares both prototype designs. The plant performance is calculated in terms of plant efficiency loss due to condenser operation as described by Equation (15) and the condenser size is plotted as condenser face area. Each data point is the efficiency loss at the optimum fan speed for the respective condenser design. For clarity purposes only the

performance at the ambient temperature of 20°C are plotted but the general trend remains constant despite the ambient temperature. The plot shows that the four row design offers significant efficiency savings over the initial six row design. This result demonstrates the higher heat rejection-to-fan power consumption ratio of the four row design. While there is a decrease in heat transfer area, the reduction in fan power consumption is far more significant. For both designs, as the condenser size increases, a decrease in efficiency-loss is achieved due to the fact that the heat transfer area increases and the required fan speed reduces, reducing the total fan power consumption. However, increasing the condenser size also increases capital costs and footprint area. In some cases, particularly solar plants with a central tower, space is limited for a large condenser. Therefore there is a trade-off between efficiency, cost and available footprint area at the plant location.

Figure 6 presents the results of the cost-efficiency analysis which offers a more effective means of comparing the two condenser prototypes. The capital cost was estimated using Equation (16). The efficiency loss due to condenser operation is plotted against the cost and for any given capital cost, the four row design offers over one percent increase in plant efficiency compared to the six row design. This is a significant improvement in terms of the overall plant performance.

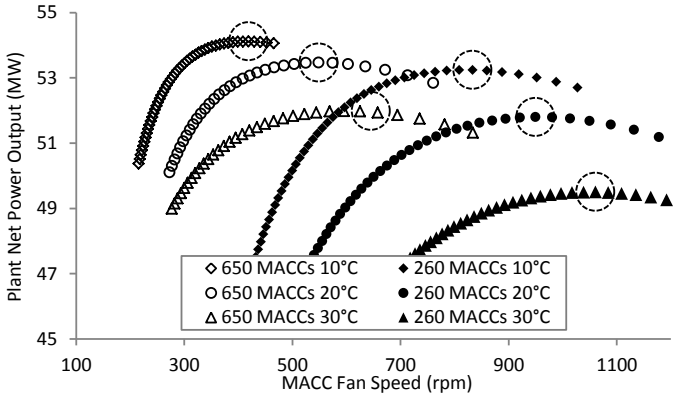

Figure 4. A plot of plant net output power plotted against MACC fan speed for two condenser sizes (no. of MACCs) and a range of ambient temperatures

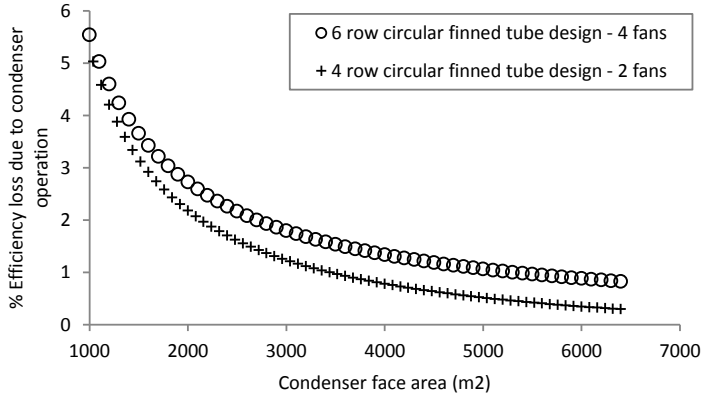

Figure 5. The efficiency loss due to condenser operation plotted against the condenser face area

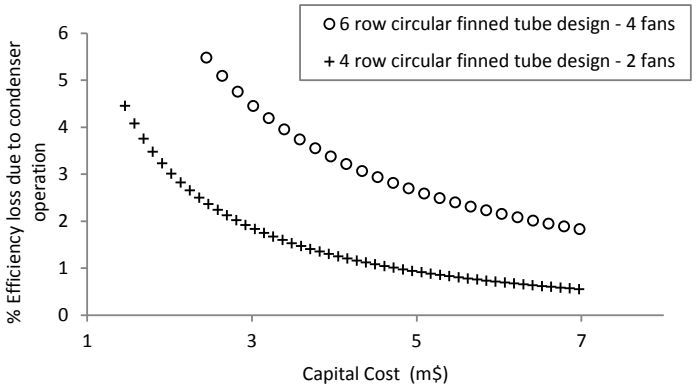

Figure 6. The efficiency loss due to condenser operation plotted against the forecasted capital cost of the respective designs

6. Conclusions

- A full-scale prototype test facility to characterize the thermal and aerodynamic performance was designed and commissioned
- The use of various correlations developed by [4, 7, 10] to predict the heat transfer and pressure drop through the condenser were verified
- The measurements show there is negligible difference in thermal performance between forced and induced draft condenser for a six and four row condenser design
- A thermodynamic model to investigate the effect of condenser design on CSP plant net output power was developed
- The four tube row condenser offers substantial improvements against the six row condenser in terms of plant thermodynamic efficiency and also the cost efficiency

Acknowledgements

The research leading to these results has received funding from the European Union's Seventh framework Programme (FP7/2007-2013) under grant agreement number 256797 as part of the MACCSol project [17]. The consortium of project partners consists of three universities and four industrial partners. The universities are the University of Limerick in Ireland, the University of Erlangen in Germany and the University of Perugiain Italy. The industrial partners involved are R&R Mechanical Ltd. in Ireland, Torresol Energy Investments Ltd. in Spain, AuBren Ltd in Ireland and the Electricity Authority of Cyprus.

References

[1] Walsh, E.J., Grimes, R., Griffin, G., 2011, Flow distribution measurements from an air cooled condenser in a 400MW power plant, *prod ASME IMECE 2011*

[2] Zukauskas, A. Heat Transfer from Tubes in Crossflow, *Adv. In Heat Transfer*, Vol. 18, Elsevier

[3] Nir. A, Heat Transfer and Friction Factor Correlations for Crossflow over Staggered Finned Tube Banks, *Heat Transfer Engineering*, Vol. 12, Issn. 1, 1991, pp. 43-58

[4] Gianolio, E. & Cuti, F., Heat Transfer and Pressure Drop for Air Coolers with Different Numbers of Rows Under Induced and Forced Draft, *Heat Transfer Engineering*, Vol. 3, Issn. 1, 1981, pp.38-48

[5] Moore, J., Grimes, R. and Walsh E., Performance analysis of a modular air cooled condenser for a concentrated solar power plant, *Proceedings IMECE2012, 2012,* Houston, TX, USA

[6] O'Donovan, A., Grimes, R., Walsh, E., Moore, J. and Reams, N., Steam-Side Characterisation of a Modular Air-Cooled Condenser, *Proceedings IMECE2012, 2012* Houston, TX, USA
[7] Robinson, K.K., and Briggs, D.E., Pressure drop of air flowing across triangular pitch banks of finned tubes, *Chem. Eng. Prog. Symp. Ser.*, 62(64), 1966, 1987, 177-183
[8] Kays, W.M. and London, A.L., Compact Heat Exchangers, 1998, Keieger Publishing Company, Florida, USA
[9] Shah, R.K. and Sekulic, D.P., Fundamentals of heat exchanger design, Wiley, New Jersey, 2003
[10] Briggs, D.E., and Young, E.H., Convective heat transfer and pressure drop of air flowing across triangular pitch banks of finned tubes, *Chem. Eng. Prog. Symp. Ser.*, 59(41), 1963, 1-8
[11] Osbourne, W.C., Fans, 2nd Edition, 1977, Pergamon Press, Oxford
[12] Berry, C.H., Flow and Fan – Principles of Moving Air through Ducts, 2nd Edition, 1963, The Industrial Press, New York
[13] Kays, W.M. and London, A.L., Heat Transfer and Friction Characteristics of Some Compact Heat-Exchanger Surfaces Part 1-Test System and Procedure, *Trans. ASME*, vol. 72, 1956, pp.1075-1056
[14] Wang, C.C, Webb, R.L. and Chi, K.Y., Data reduction for air-side performance of fin-and-tube heat exchangers, Experimental Thermal and Fluid Science, Vol. 21, 2000, pp. 218-226
[15] Gardner, K.A., Mean temperature difference in an array of identical heat exchangers, *Ind. Eng. Chem.*, 34, 1942, 1083-1087
[16] Poullikkas, A., Grimes, R., Walsh, E.J., Hadjipaschalis, I. and Kourtis, G., Optimization analysis of innovative modular air-cooled condensers for CSP plants, *2012*
[17] Meyer, C.J. and Kröger, D.G., Plenum chamber flow losses in forced draught air-cooled heat exchangers, Journal of Applied Thermal Engineering, Vol. 18, 1998, P.875-893